NASA
TN
D-5744
[pt.4]
c.1

NASA TECHNICAL NOTE

NASA TN D-6568

NASA TN D-6568

DESIGN STUDY OF SHAFT FACE SEAL WITH SELF-ACTING LIFT AUGMENTATION

IV - Force Balance

by Lawrence P. Ludwig, John Zuk, and Robert L. Johnson

Lewis Research Center
Cleveland, Ohio 44135

NATIONAL AERONAUTICS AND SPACE ADMINISTRATION • WASHINGTON, D. C. • APRIL 1972

1. Report No. NASA TN D-6568	2. Government Accession No.	3. Recipient's Catalog No.
4. Title and Subtitle DESIGN STUDY OF SHAFT FACE SEAL WITH SELF-ACTING LIFT AUGMENTATION IV - FORCE BALANCE		5. Report Date April 1972
		6. Performing Organization Code
7. Author(s) Lawrence P. Ludwig, John Zuk, and Robert L. Johnson		8. Performing Organization Report No. E-6458
		10. Work Unit No. 132-15
9. Performing Organization Name and Address Lewis Research Center National Aeronautics and Space Administration Cleveland, Ohio 44135		11. Contract or Grant No.
		13. Type of Report and Period Covered Technical Note
12. Sponsoring Agency Name and Address National Aeronautics and Space Administration Washington, D.C. 20546		14. Sponsoring Agency Code

15. Supplementary Notes

16. Abstract

A method for predicting the operating film thickness of self-acting seals is described. The analysis considers a 16.76-cm (6.60-in.) mean diameter seal that is typical of large gas turbines for aircraft. Four design points were selected to cover a wide range of operation for advanced engines. This operating range covered sliding speeds of 61 to 153 m/sec (200 to 500 ft/sec), sealed pressures of 45 to 217 N/cm^2 abs (65 to 315 psia), and gas temperatures of 311 to 977 K (100° to 1300° F). The force balance analysis revealed that the seal operated without contact over the operating range with gas film thicknesses ranging between 0.00046 to 0.00119 cm (0.00018 to 0.00047 in.), and with gas leakage rates between 0.01 to 0.39 scmm (0.4 to 14.0 scfm).

17. Key Words (Suggested by Author(s)) Mechanical seal Force balance	18. Distribution Statement Unclassified - unlimited		
19. Security Classif. (of this report) Unclassified	20. Security Classif. (of this page) Unclassified	21. No. of Pages 28	22. Price* $3.00

* For sale by the National Technical Information Service, Springfield, Virginia 22151

DESIGN STUDY OF SHAFT FACE SEAL WITH SELF-ACTING LIFT AUGMENTATION
IV - FORCE BALANCE

by Lawrence P. Ludwig, John Zuk, and Robert L. Johnson
Lewis Research Center

SUMMARY

Self-acting face seals, because of noncontact operation, have high-speed potential. The lift force of the self-acting geometry provides positive gas film stiffness, which allows the nosepiece to dynamically track (without rubbing) the runout motions of the seat face. Further, the self-acting seal can operate with a small separation (film thickness) of the sealing surface; thus, mass leakage flow through the seal is similar to that usually associated with a contact seal. The magnitude of the film thickness is determined by the seal force balance: too large a film (e.g., 0.0025 cm, or 0.0010 in.) results in excessive leakage and nosepiece vibration; too small a film (e.g., 0.00025 cm, or 0.0001 in.) results in a seal with little tolerance to thermal deformation. Therefore, the force balance of the seal must be accurately determined and adjusted in order to establish acceptable operating film thickness. However, the conventional method of seal force balance is inadequate since it provides no insight to film thickness and leakage. A procedure that predicts operating film thicknesses is described.

The factors considered in the force balance were (1) the mechanical spring force, (2) the pneumatic closing force due to the sealed pressure, (3) the pneumatic opening force due to the sealed pressure, and (4) the self-acting force generated by the lift pads. The ranges of operating conditions were 61 to 153 meters per second (200 to 500 ft/sec) sliding speed, 45 to 217 N/cm^2 abs (65 to 315 psia) sealed pressure, and 311 to 977 K (100° to 1300° F) sealed gas temperature.

In the analysis, the seal size was typical of that for large gas turbine engines (e.g., 16.76-cm (6.60-in.) mean seal diameter). Operating film thicknesses and resulting gas leakages were determined by establishing the force balance for four design points that represented a wide range of hypothetical conditions in advanced aircraft gas turbines.

The force balance analysis predicted noncontact operation for all four design points. The equilibrium film thicknesses were between 0.00046 and 0.00119 centimeter (0.00018 and 0.00047 in.) for the range of operating conditions. The calculated leakages for these film thicknesses ranged between 0.01 and 0.39 scmm (0.4 and 14.0 scfm) for the four design points. Thus, noncontact operation with acceptable gas leakage rates are predicted over the range of design points that covered a wide range of hypothetical engine operation conditions.

INTRODUCTION

Shaft face seals for advanced turbine engines for aircraft have received considerable research and development effort aimed at extending seal speed and pressure capability (ref. 1). In particular, seals with self-acting lift augmentation (refs. 2 and 3) promise a seal with the rotating speed capability of labyrinth seals and the low leakage capability of contact seals. This self-acting lift seal (described in ref. 4) is similar in construction to a conventional face seal except for the addition of a self-acting geometry that acts to keep the primary faces separated. Thus, the seal has high-speed potential. For ideal operation, rubbing would occur only on startup and shutdown. The lift force of the self-acting geometry provides positive gas film stiffness (ref. 5), which allows the nosepiece to dynamically track the runout motions of the seat face. Further, the self-acting geometry tends to operate with a small separation of the primary faces. For this reason, the mass leakage flow through the primary seal can be much less than that of a labyrinth seal (ref. 6).

Of particular interest is the magnitude of the separation of the primary seal faces (operating gas film thickness). If the operating gas film thickness is too large (e.g., 0.0025 cm or 0.0010 in.), the gas leakage is excessive. Furthermore, in experimental studies (ref. 7) it has been demonstrated that with large film thicknesses and associated low film stiffness, the primary ring does not properly track the motions of the seat face. This dynamic instability places an upper limit on useful seal rotational speed and seat face runout. On the other hand, if no operating gas film is established, the rubbing contact would cause excessive wear at high speeds (i.e., above 107 m/sec, or 350 ft/sec). Furthermore, if the film thickness is small (e.g., less than 0.00025 cm, or 0.0001 in.), the seal has little tolerance to face deformation. Thus, the practical operating film thickness spans a range of approximately 0.00025 to 0.00127 centimeter (0.0001 to 0.0005 in.).

Since the practical range of film stiffness is small (being limited on one end by tolerance to face deformation and on the other end by leakage and dynamic considerations), it is necessary in the design process to accurately predict the operating film thicknesses. This gas film thickness is determined by the forces acting on the primary ring.

In conventional seal design practice the process of controlling these forces on the primary ring is called pressure balancing. In current face seal technology the degree of pressure balancing is expressed by an area ratio (ref. 8). This is the net area over which the seal pressure acts to close the seal divided by the area of the primary seal. This practice does not provide any insight to operating film thickness and leakage; but it does provide an approximate indicator as to the magnitude of the net force tending to close the seal.

To determine film thicknesses and leakage in a self-acting seal, the axial force acting on the primary ring must be determined for each operating condition. These forces are comprised of the self-acting lift pad force, the spring force, and the pneumatic forces due to the sealed pressure. Essentially, the analysis requires finding the film thickness for which the opening forces balance the closing forces. When this equilibrium film thickness is known, leakage can be calculated. It should be noted that this force balance procedure is for the case in which the seat face has zero runout with respect to the shaft centerline. Seat face runout introduces dynamic film thickness changes, as discussed in reference 7.

Detailed studies (refs. 4 to 6) have been made on self-acting and pneumatic pressure forces in self-acting seals. These analyses were used in this work to establish the seal force balance and resulting film thickness with associated leakage. The overall objective of this work is to determine seal force balances that will be suitable for various engine operating conditions. The particular objectives are (1) establish a procedure for investigating force balance in self-acting seals, (2) determine if the seal will operate without rubbing contact over the range of gas turbine engine conditions by calculating the seal force balance and resulting operating film thickness, and (3) calculate seal leakage rates over a wide range of engine operating conditions.

The seal design used in this analysis is fully described in reference 4. The mean seal diameter of 16.76 centimeters (6.60 in.) is typical of the size necessary for large gas turbine aircraft engines. Force balance and leakage were determined at four design points: idle, takeoff, climb, and cruise. This range of operation is hypothetical and was selected to cover a wide range of conditions in engines. The conditions covered are sliding speeds of 61 to 153 meters per second (200 to 500 ft/sec), sealed pressures of 45 to 217 N/cm^2 abs (65 to 315 psia), and sealed air temperatures of 311 to 977 K (100° to 1300° F). The self-acting force was determined by the computer program given in reference 5, and the pressure profile across the sealing dam was analyzed by the computer program described in reference 9.

APPARATUS

Self-Acting Seal Assembly

Figure 1 shows the seal assembly, and figure 2 gives the nomenclature that applies to the self-acting seal. As with a conventional face seal, it consists of a rotating seat that is attached to the shaft and a nonrotating primary ring assembly that moves in an axial direction and, thus, accommodates engine thermal expansion (axial). The secondary ring (piston ring) is subjected only to the axial motion (no rotation) of the primary ring

assembly. Several springs provide mechanical force to maintain contact at start and stop. In operation, the sealing faces are separated a slight amount (in the range of 0.00025 to 0.00127 cm, or 0.0001 to 0.0005 in.) by action of the self-acting lift geometry, and gas leakage flow is from the high-pressure side (inside diameter of carbon primary ring) between the primary sealing faces into the bearing sump.

The primary ring assembly contains a carbon-graphite ring that is shrink fitted into a molybdenum retainer ring. This primary ring, in turn, is located radially by a resilient piloting ring attached to the carrier. This resilient ring and the static seal between the carbon-graphite ring and the carrier are important features in prevention of thermal deformation. The resilient ring is flexible enough to allow differential thermal growth between the carrier and the primary ring. And since the surfaces forming the static seal (see fig. 2) can move radially relative to each other, coning deformation is not induced into the primary ring. (See ref. 4 for a detailed description of this seal and its nomenclature.)

The axial forces acting on the primary ring are shown in figure 3 (high pressure on the inside diameter of the seal). They consist of

   (1) A mechanical spring force
   (2) A pneumatic closing force (due to the sealed pressure)
   (3) A pneumatic opening force (due to the sealed pressure)
   (4) A self-acting force (generated by the lift pads)
From an overall viewpoint, the pneumatic forces are balanced such that a small net pneumatic closing force exists; and the self-acting geometry provides enough force to overcome the spring force and this small net pneumatic closing force. Thus, separation of the surfaces is achieved.

In investigating seal force balance, the effect of nonparallel primary seal faces must also be considered. Nonparallel faces are illustrated in figure 4. The important point is that nonparallel faces affect the force produced by the self-acting geometry and also the pressure gradient between the primary seal faces. These nonparallel effects on self-acting geometry are discussed in reference 5.

In this report the force balance will first be established for parallel surfaces at the design operating points. Then a design point will be chosen to illustrate the effects of nonparallel operation. Also, it should be restated that the analysis presented in this report is for operation in which the seat face has zero runout and, consequently, the film thickness is not dependent on time. However, in actual operation, the seat face will always have some face runout that causes the film thickness to vary with time (ref. 7). Despite this time dependence the zero runout analysis yields useful data and insight on the seal performance.

Force Balance

In current seal technology, an area ratio (net area on which sealed force acts divided by the area of the primary seal) is often used to indicate the extent to which the pneumatic (or hydraulic) forces have been balanced out. For example, seal manufacturers often use the degree of balance shown in figure 5 (defined in ref. 8). Figure 5(a) shows a seal with a high closing force. Here the sealed pressure acts on an area equal to the primary seal area. Therefore, the area ratio is 1.0. As another example, figure 5(b) shows a seal in which the closing force acts over an area equal to 65 percent of the primary seal area. This seal will generally have a slight closing force which is near that sometimes used for conventional face seals for sealing a gas.

Geometric ratios such as the preceding can provide an indicator for the extent to which the forces are balanced out. However, as mentioned previously, this geometric relation does not provide insight as to film thickness and consequent leakages in self-acting seals. What is required is an accurate determination of the forces acting on the primary ring. In particular, the shape of the pressure gradient in the primary seal must be calculated for the various operating points, and the effect of face deformation must be evaluated.

Design Points

Past experience (ref. 1) has shown that conventional seals are difficult to pressure balance over a wide range of operation. That is, a pressure balance suitable for high pressure may be inadequate for lower pressure and the opposite. Therefore, four seal operating points were selected to cover the wide operation range of advanced engines. These points, which represent hypothetical idle, cruise, takeoff, and climb, are shown in table I. The seal force balance was determined for each design point. And an alternate mechanical spring force was selected to show its effect on operating film thickness.

Secondary Seal

The secondary seal is a metal piston-ring type and is shown in figures 2 and 6. Forces acting in this ring arise principally from the sealed air pressure. By grooving the side and ring outside diameter, the force due the sealed air can be partially balanced. From a practical standpoint complete force balance cannot be obtained; therefore, axial frictional force acts on the outside diameter of the piston ring. The direction of this force always opposes motion of the primary ring assembly. Studies

(ref. 7) on self-acting seals revealed that the primary ring motion can closely match that of the seat mating face. (The seat mating face motion is a nutation due to face out-of-squareness with respect to the shaft centerline.) Typical face runout values are 0.0025 to 0.0076 centimeter (0.001 to 0.003 in.) full indicator reading for a 16.76-centimeter (6.60-in.) diameter seal. This motion is accommodated by the secondary seal; hence, fretting wear is often a problem. Since the motion is a nutation, the net axial force per revolution is zero; but the frictional resistance produced by the secondary ring is a rotating (at shaft frequency) couple that acts as a damping force. These frictional forces are not considered in the axial force balance presented in this report. However, these frictional effects can significantly affect the primary ring dynamic response. Some preliminary analysis reveals that the piston ring damping causes the primary sealing faces to have angular misalinement with respect to each other; more work is needed in the area.

Primary Seal Mathematical Model

In calculating the axial force balance of the primary ring, the pressure gradient in the primary seal must be considered (see fig. 2 for primary seal location). The quasi-one-dimensional flow model described in reference 9 was used for these calculations. From a gas leakage flow standpoint, the primary seal is a long narrow slot. For example, a typical operating film thickness of a self-acting seal is in the range of 0.00102 centimeter (0.0004 in.), and a typical radial length of the primary seal is 0.127 centimeter (0.050 in.). Thus, the length-height ratio of the flow channel is 125/1. Previous work (refs. 10 and 11) has shown that this narrow slot has the following qualitative features:

(1) Laminar leakage flow prevails for the range of interest in seals for gas turbines (pressure range to 217 N/cm^2 abs (315 psia)).

(2) Sonic velocity (choking) exists at the slot exit when pressure ratios are approximately 4/1 or greater at a mean film thickness of 0.00102 centimeter (0.0004 in.).

(3) Pressure profiles for choked and nonchoked flow can be very different.

(4) Since the primary seal radial width is small compared with its diameters, the area expansion effect on flow can be ignored.

(5) The leakage flow and pressure profile are significantly different if the surfaces of the primary seal are not parallel. (See ref. 3 for a discussion of the effects of converging and diverging sealing surfaces.)

The mathematical model used in the quasi-one-dimensional analysis of reference 9 is shown in figure 7. Since area expansion effects are ignored, the model is a narrow slot of height h and length l.

The following restrictions apply to the mathematical model (see ref. 9 for details):

(1) Effect of rotation on flow is neglected.

(2) For subsonic flow below a Mach number of $1/\sqrt{\text{Specific-heat ratio}}$, the flow is isothermal and the model yields the classical cubic dependence of mass flow on film thickness.

(3) For flow greater than a Mach number of $1/\sqrt{\text{Specific-heat ratio}}$, the viscous effects are approximated by a mean friction factor of $24/(\text{Reynolds number})$.

Primary Seal Opening Force

The force in the primary seal that tends to open the seal was calculated by the method described in reference 9. Typical pressure gradients across the primary seal (for design points 1 and 3) are shown in figure 8. The important point is that choked and nonchoked flows can have pressure gradients with very different shapes. The integrated force under this pressure-gradient curve constitutes the opening force, and figure 9 shows this primary seal opening force as a function of film thickness for the four design points. Note that for all four design operating points, the opening force is nearly independent of film thickness.

Primary Seal Leakage

The primary seal leakage as a function of film thickness is shown in figure 10. Here leakage is plotted for the four design points from table I. The mathematical model described in reference 9 was used for these calculations. In general, the flow is choked (sonic velocity at exit) except for the very small film thickness. It should be emphasized that these calculated values are for parallel surfaces. The effects of nonparallel surfaces are considered later for design point 2.

Self-Acting Geometry

Self-acting geometry mathematical model. - The self-acting lift pads consist of a series of shallow recesses 0.0025 centimeter (0.001 in.) deep arranged circumferentially around the seal under the sealing dam, as shown in figure 11. An important point is that the lift pads are bounded at the inside diameter and the outside diameter by the sealed pressure P_1. (This is accomplished by feed slots connecting the annular groove directly under the primary seal face.) Therefore, a pressure gradient due to gas leak-

age occurs only across the primary seal. This is an important point in minimizing the effects of face deformation.

The complete primary ring and its 20 lift pads are shown in figure 12. And as indicated in figure 12, motion of the rotor over these shallow recesses drags air from the feed slots into the shallow pad recesses. Since the air is restricted from leaving the recesses by the side and back lands, a lift force, or thrust bearing action, is produced.

This self-acting lift pad is approximated by the mathematical model shown in figure 13. Note that the curvature effects have been neglected in the model. Therefore, the model corresponds to a Cartesian coordinate system.

This mathematical model is described in detail in reference 5. In this analysis the following restrictions apply:

(1) The fluid is Newtonian and viscous.

(2) A laminar flow regime is assumed.

(3) Body forces are negligible.

The analysis of reference 5 admits nonparallel surfaces; thus, the effects of surface deformation on lift force can be evaluated.

Self-acting opening force. - Figure 14 shows the lift force produced by the self-acting geometry for the four operating points of table I. These lift-force-against-film-thickness curves were calculated by the method described in reference 5. This lift force tends to open the seal and is added to the primary seal opening force to obtain the total opening force. The resulting combined opening force given in figure 15 is obtained by combining figures 9 and 14. Again this is for parallel surfaces only.

Primary Ring Closing Forces

The closing forces (see fig. 16) acting on the primary ring are a spring force and a pneumatic force. Since the full sealed pressure acts to the inside diameter of the primary seal, the net pneumatic closing force acts only on the annular area between the primary-seal inside diameter and the secondary-seal outside diameter. For the seal design, this annular area is (see fig. 16):

$$A = \frac{\pi}{4}\left(D_1^2 - D_2^2\right) = 4.66 \text{ cm}^2 (0.72 \text{ in.}^2)$$

The closing forces due to the sealed pressure are listed in table II. The closing forces in table II are for average dimensions at room temperature. At operating temperature a thermal growth difference may have caused a change in the relation between the

secondary-seal outside diameter and the inside diameter of the primary seal. Thus, the closing force could be a function of temperature. However, in the design under discussion the thermal effects were not significant, as shown in figure 17, which is a thermal map of the primary seal ring. Therefore, in this report all force balance calculations were based on room-temperature dimensions.

Seal Force Balance

In a conventional seal, the net closing force is resisted by solid-surface rubbing contact; thus, a total force balance is achieved. But in self-acting seals the force balance is achieved without rubbing contact. Therefore, for a given design point, the seal will operate at a film thickness such that the total opening force exactly balances the total closing force. This operating film thickness is obtained by plotting total opening forces (fig. 15) and total closing forces (table II) as a function of film thickness. The intersection (see fig. 18) of these curves is the equilibrium (operating) film thickness. This film thickness determination does not take into account dynamic running factors such as seat face runout (see ref. 7) and piston ring damping. Once the operating film thickness is found, the calculated leakage can be determined by reference to figure 10. For the four design points, table III shows the equilibrium film thickness and calculated leakage for this film thickness.

Force Balance Indicators

As previously noted, an area ratio is the conventional method of expressing the degree to which the force due to sealed pressure is balanced (fig. 5). This area ratio is not exact since the pressure profile shape in the primary seal depends on pressure ratio (see fig. 8). Table IV shows a comparison between the conventional force balance indicator (area ratio) and the proposed force ratio indicator. This force ratio indicator is closing force due to sealed pressure divided by opening force due to sealed pressure. The area ratio is, of course, constant for all design points. However, the force ratio varies (see table IV). And this is because of the different pressure profile shapes for each design point. Note that the net closing force due to the sealed pressure is small (8.9 to 20.8 N, or 4.7 to 2.0 lbf) at the four design points. Thus, the self-acting pads act, principally, against the spring force in this particular design.

Of course, the seal designer has the option of varying the portion of the closing force that is due to springs. He may choose to use more spring force and less force due to the sealed pressure. This choice depends somewhat on the range of operating

conditions that must be accommodated. The important point is that each operating point should be checked for equilibrium film thickness. If these film thicknesses are not satisfactory, the force balance should be altered to bring all operating points within a satisfactory film thickness regime. Experience has shown that the satisfactory film thickness regime is about 0.00025 centimeter (0.0001 in.) on the low end (some tolerance to thermal deformation must be maintained) and 0.0012 centimeter (0.0005 in.) on the high end. These limits are only approximate and depend to a large extent on the dynamic and thermal condition to which the seal is subjected. The high limit of practical film thickness is established by seal dynamics and leakage considerations. In particular, the primary ring response to the seat face runout becomes excessive as the mean film thickness increases (ref. 7). This is because the stiffness of the gas film decreases with increasing film thickness.

For an existing set of seal hardware, the film thickness is most easily changed by increasing or decreasing the spring force. The effect of this can be seen in figure 19, which shows what happens to the equilibrium film thicknesses (of fig. 18) when the spring force is increased from 71.2 newtons (16 lbf) to 115.6 newtons (26 lbf). As shown in figure 19, an increase of 44.5 newtons (10 lbf) causes the film thickness to decrease about 30 percent for design point 1.

Startup and stop operation requirements are another consideration in selecting the amount of closing force due to sealed pressure and the amount of closing force due to the spring. Experience (ref. 7) has shown that adverse rubbing contact can occur during startup (or shutdown) under the condition of no pressure and light spring loads. This rubbing contact is in the form of a nutation and is induced by low gas film stiffness (ref. 7). Fortunately, in a gas turbine engine, the pressure increases as the speed increases (not linearly) and the condition of high rotation speed and low pressure is not of concern.

Effect of Nonparallel Seat Face

Figure 4 shows, in an exaggerated manner, the coning displacement of the seal seat. (The primary ring could also be coned.) This type of coning displacement, which can be caused by thermal gradients, results in nonparallel faces within the primary seal and the self-acting geometry. These nonparallel faces have a significant effect on load capacity of the self-acting geometry; also the primary seal opening force is affected. Thus, in design, the equilibrium operating film thickness should be calculated for anticipated coning displacements.

As a example of the effect of this coning, design point 2 was checked for equilibrium film thickness for a distortion of 0.0013 centimeter (0.0005 in.) across the self-acting

10

pad. This is a distortion of 2 milliradians and is severe as judged by seal operation experience (ref. 1). Figure 20 shows this assumed distortion in an exaggerated manner; note that the self-acting pad and primary seal dimensions are given.

Figure 21 shows the self-acting lift force for the 2-milliradian distortion of the seat face. Note that the force is plotted as a function of the mean film thickness of the self-acting pad. Also plotted, for comparison, is force generated for a parallel film (a repeat of the data in fig. 14).

As noted previously, the primary seal opening force is also affected by nonparallel faces; and this was calculated by using an analysis similar to reference 12 for the 2-milliradian distortion. The results are given in figure 22. Note that for the divergent deformation shown in figure 22, there is a marked reduction in load as the film thickness decreases. For convergent deformation, the load would increase as film thickness decreases and this is desirable. Unfortunately, in aircraft engines, the divergent deformation is a natural tendency due to thermal gradients.

Finally, in figure 23, the equilibrium film thickness is found by finding the intersection between the total closing force and total opening force. A spring force of 71.2 newtons (16 lbf) was used for this purpose.

With the equilibrium film thickness values, the gas leakage was calculated by using the method described in reference 12. And the results for design point 2 reveal that the leakage rate for the 2-milliradian deformation was nearly twice that of the parallel-face case.

SUMMARY OF RESULTS

The force balance and resulting operating film thickness are determined for a self-acting lift pad seal of the size (approx. 16.76 cm, or 6.60 in.) typical for large gas turbines for aircraft. The four design points considered covered a hypothetical range of operation for advanced engines. The range of operation included sliding speeds of 61 to 153 meters per second (200 to 500 ft/sec), gas temperatures of 311 to 977 K (100° to 1300° F), and pressure differentials of 45 to 217 N/cm^2 abs (50 to 300 psia). Analysis was made of forces acting on the primary ring by using the following assumptions:

(1) Isothermal seal structure at room temperature

(2) Steady-state operation with zero seat face runout

(3) No axial force at the secondary seal

An analytical procedure was developed for prediction of operating film thicknesses and resulting leakage in self-acting seals. In particular, this analysis revealed the following:

1. Noncontact operation with acceptable leakage is predicted at the selected four design conditions of idle, takeoff, climb, and cruise.

2. The operating film thickness ranged between 0.00046 and 0.00119 centimeter (0.00018 and 0.00047 in.) for the four design conditions.

3. The calculated seal leakage rates ranged between 0.01 and 0.39 scmm (0.4 and 14.0 scfm) for the four design conditions.

4. For a typical operating condition, noncontact operation was predicted under the assumption of a 2-milliradian face deformation. Gas leakage was about twice that for parallel-face operation.

Lewis Research Center,
   National Aeronautics and Space Administration,
      Cleveland, Ohio, January 20, 1972,
         132-15.

REFERENCES

1. Parks, A. J.; McKibbin, R. H.; and Ng, C. C. W.: Development of Main-shaft Seals for Advanced Air Breathing Propulsion Systems. Rep. PWA-3161, Pratt & Whitney Aircraft (NASA CR-72338), Aug. 14, 1967.

2. Johnson, Robert L.; Loomis, William R.; and Ludwig, Lawrence P.: Performance and Analysis of Seals for Inerted Lubrication Systems of Turbine Engines. NASA TN D-4761, 1968.

3. Johnson, Robert L.; and Ludwig, Lawrence P.: Shaft Face Seal with Self-Acting Lift Augmentation for Advanced Gas Turbine Engines. NASA TN D-5170, 1969.

4. Ludwig, Lawrence P.; and Johnson, Robert L.: Design Study of Shaft Face Seal with Self-Acting Lift Augmentation. III - Mechanical Components. NASA TN D-6164, 1971.

5. Zuk, John; Ludwig, Lawrence P.; and Johnson, Robert L.: Design Study of Shaft Face Seal with Self-Acting Lift Augmentation. I - Self-Acting Pad Geometry. NASA TN D-5744, 1970.

6. Zuk, John; Ludwig, Lawrence P.; and Johnson, Robert L.: Design Study of Shaft Face Seal with Self-Acting Lift Augmentation. II - Sealing Dam. NASA TN D-7006, 1970.

7. Hady, William F.; and Ludwig, Lawrence P.: Experimental Investigation of Self-Acting-Lift-Pad Characteristics for Main-Shaft Seal Applications. NASA TN D-6384, 1971.

8. Pape, J. G.: Fundamental Aspects of Radial-Face Seals. Rep. WTHD-17, Technische Hogeschool, Delft, Netherlands, Dec. 1969.

9. Zuk, J.; Ludwig, L. P.; and Johnson, R. L.: Compressible Flow Across Shaft Face Seals. Fifth International Conference on Fluid Sealing, paper H6, 1971.

10. Zuk, John; and Ludwig, Lawrence P.: Investigation of Isothermal, Compressible Flow Across a Rotating Sealing Dam. I - Analysis. NASA TN D-5344, 1969.

11. Zuk, John; and Smith, Patricia J.: Computer Program for Viscous, Isothermal Compressible Flow Across a Sealing Dam with Small Tilt Angle. NASA TN D-5373, 1969.

12. Zuk, John; Ludwig, Lawrence P.; and Johnson, Robert L.: Quasi-One-Dimensional Compressible Flow Across Face Seals and Narrow Slots. I - Analysis. NASA TN D-6668, 1972.

TABLE I. - DESIGN POINTS

Design point	Sealed pressure, P_1		Sealed gas temperature		Seal sliding speed	
	N/cm^2 abs	psia	K	^oF	m/sec	ft/sec
1 - Idle	45	65	311	100	61	200
2 - Cruise	148	215	700	800	153	500
3 - Takeoff	217	315	977	1300	137	450
4 - Climb	148	215	811	1000	122	400

TABLE II. - CLOSING FORCE

Design point	Pneumatic						Spring force, F_s		Total closing force, $F_t = F_p + F_s$	
	Sealed pressure, P_1		Pressure change, ΔP		Sealed-pressure closing force, F_p					
	N/cm^2 abs	psia	N/cm^2	psi	N	lbf	N	lbf	N	lbf
1 - Idle	45	65	34.5	50	160.6	36.1	71.2	16	231.7	52.1
2 - Cruise	148	215	138	200	641.0	144.1	↓	↓	711.1	160.1
3 - Takeoff	217	315	207	300	963.4	216.6			1034.6	232.6
4 - Climb	148	215	138	200	641.0	144.1	↓	↓	711.1	160.1

TABLE III. - EQUILIBRIUM FILM

THICKNESS AND GAS LEAKAGE

THROUGH PRIMARY SEAL

Design point	Equilibrium film thickness		Gas leakage	
	cm	in.	scmm	scfm
1 - Idle	0.0004	0.00018	0.008	0.3
2 - Cruise	.0011	.00044	.27	9.5
3 - Takeoff	.0012	.00047	.39	14.0
4 - Climb	.0010	.00040	.18	6.4

TABLE IV. - FORCE BALANCE INDICATORS, COMPARISON BETWEEN

PRIMARY SEAL AREA RATIOS AND RATIO OF FORCES

Design point	Area ratio (common usage)[a]	Ratio of forces due to sealed pressure (proposed usage)[b]	Net closing force due to sealed pressure[c]	
			N	lbf
1 - Idle	0.70	1.15	20.8	4.7
2 - Cruise		1.02	13.3	3.0
3 - Takeoff	↓	1.06	8.9	2.0
4 - Climb		1.03	20.0	4.5

[a]Ratio of closing force area to opening force area.
[b]Ratio of sealed-pressure closing force to sealed-pressure opening force.
[c]Closing force minus opening force.
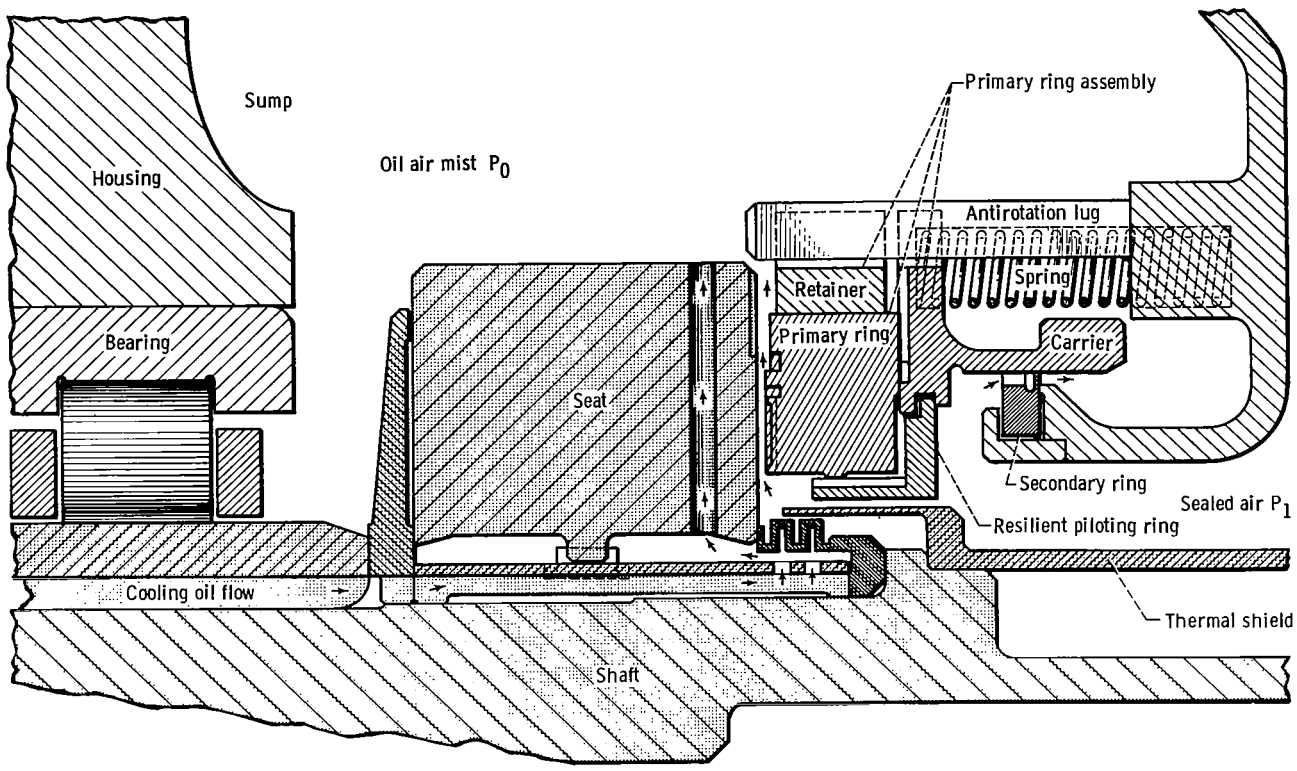
Figure 1. – Self-acting seal assembly.
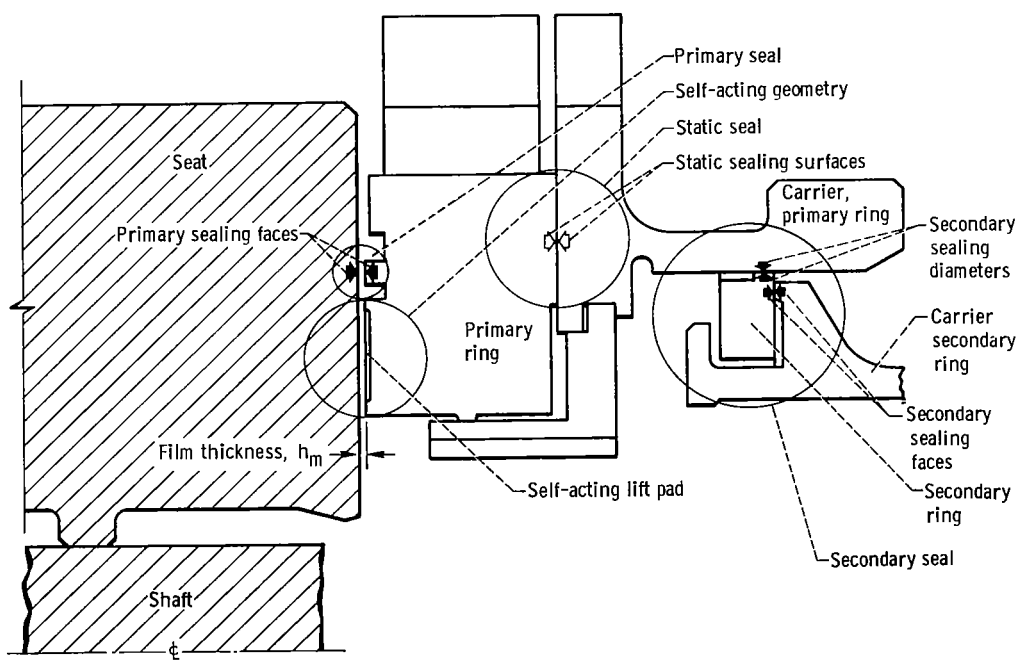
Figure 2. – Seal nomenclature for self-acting face seal.

15
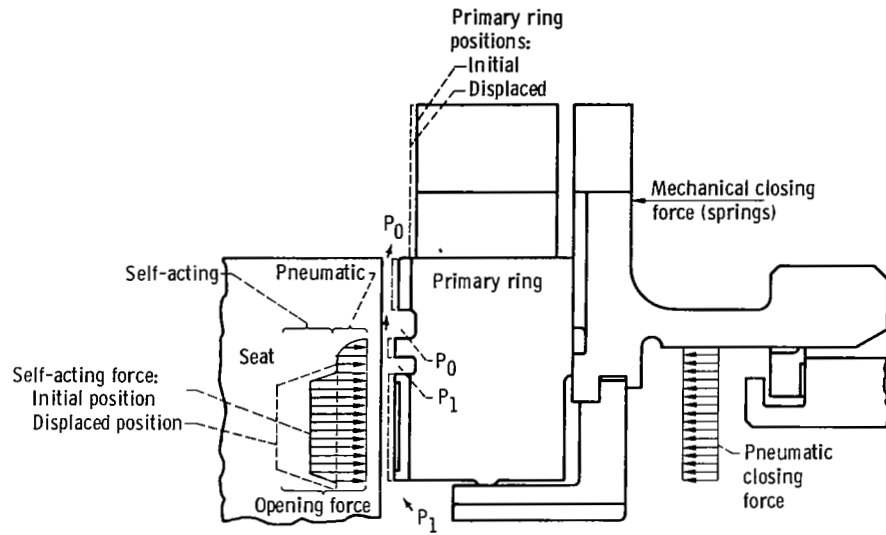
Figure 3. - Self-acting seal with mechanical, pneumatic, and self-acting forces acting on primary ring.
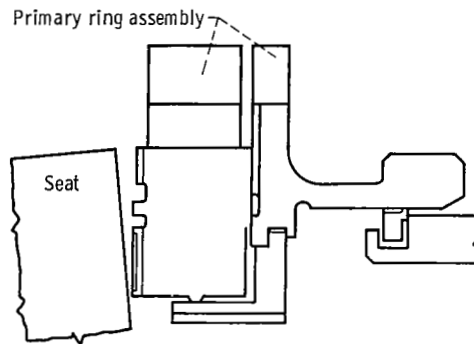
Figure 4. - Coning displacement of seat, causing non-parallel faces in primary seal and in self-acting geometry.
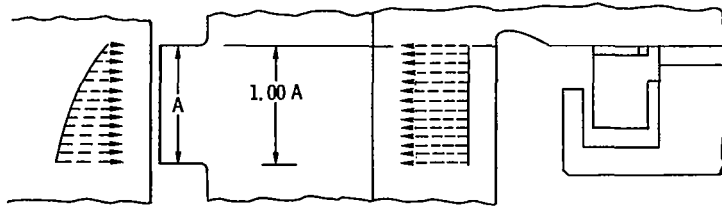
(a) Area ratio, 1.00.
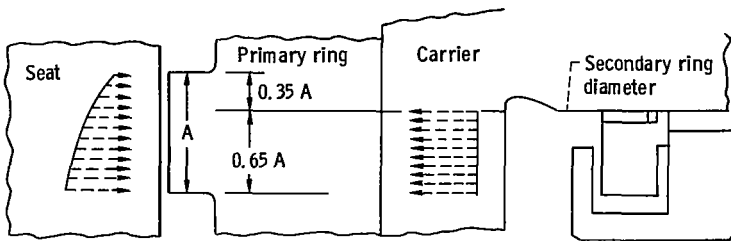
(b) Area ratio, 0.65.

Figure 5. - Area ratio use as seal force balance indicator.
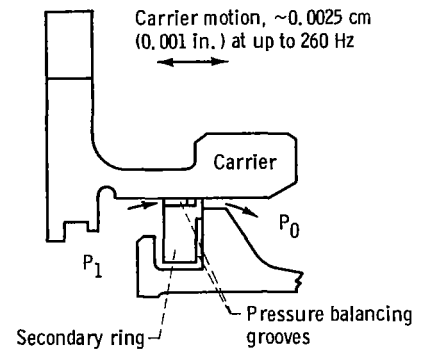
Figure 6. - Secondary seal.
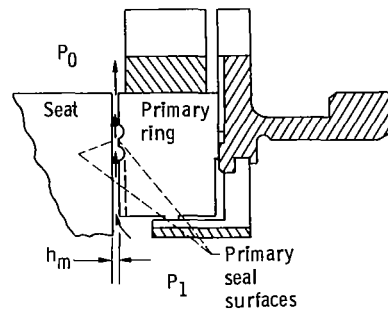
(a) Primary seal location, $P_1 > P_0$.
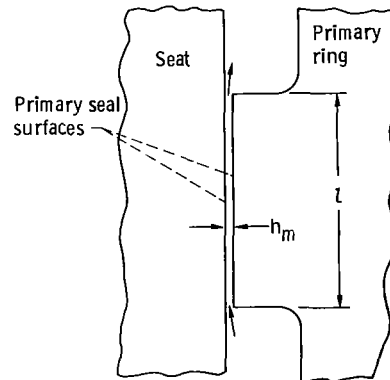
(b) Exaggerated view of primary seal.

Figure 7. - Primary seal.
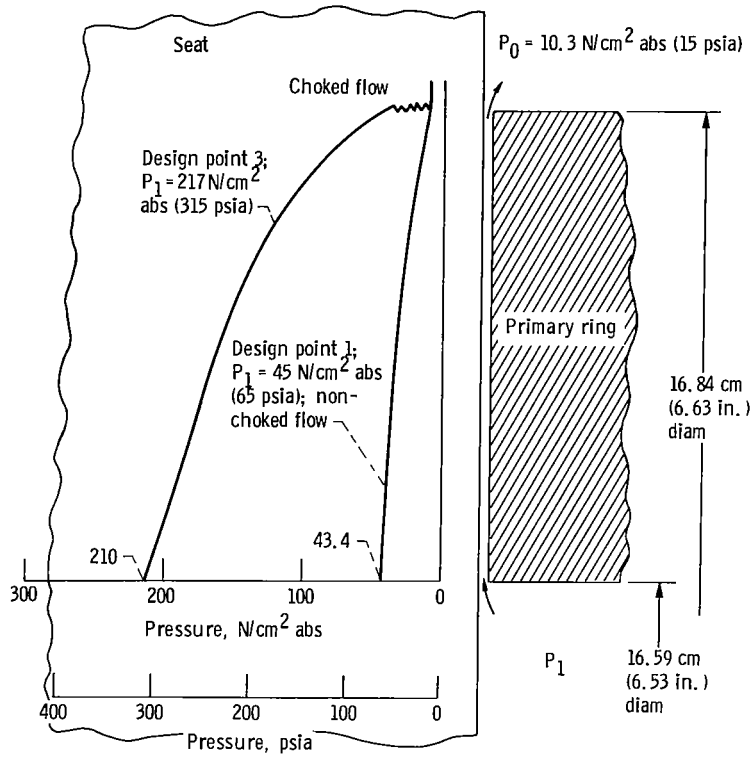
Figure 8. – Pressure gradient in primary seal, illustrating choked and nonchoked flow. Parallel face; mean film thickness h_m, 0.0010 centimeter (0.0004 in.).
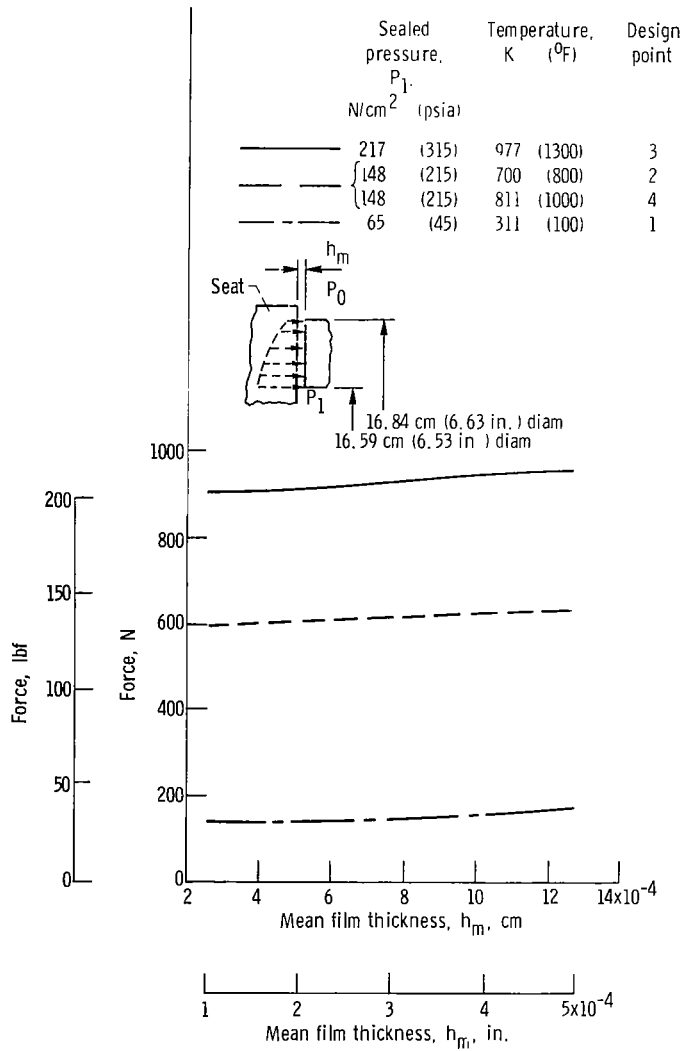
Figure 9. – Opening force acting on primary sealing face. Fluid, air; sump pressure P_0, 10.3 N/cm^2 abs (15 psia); parallel faces.
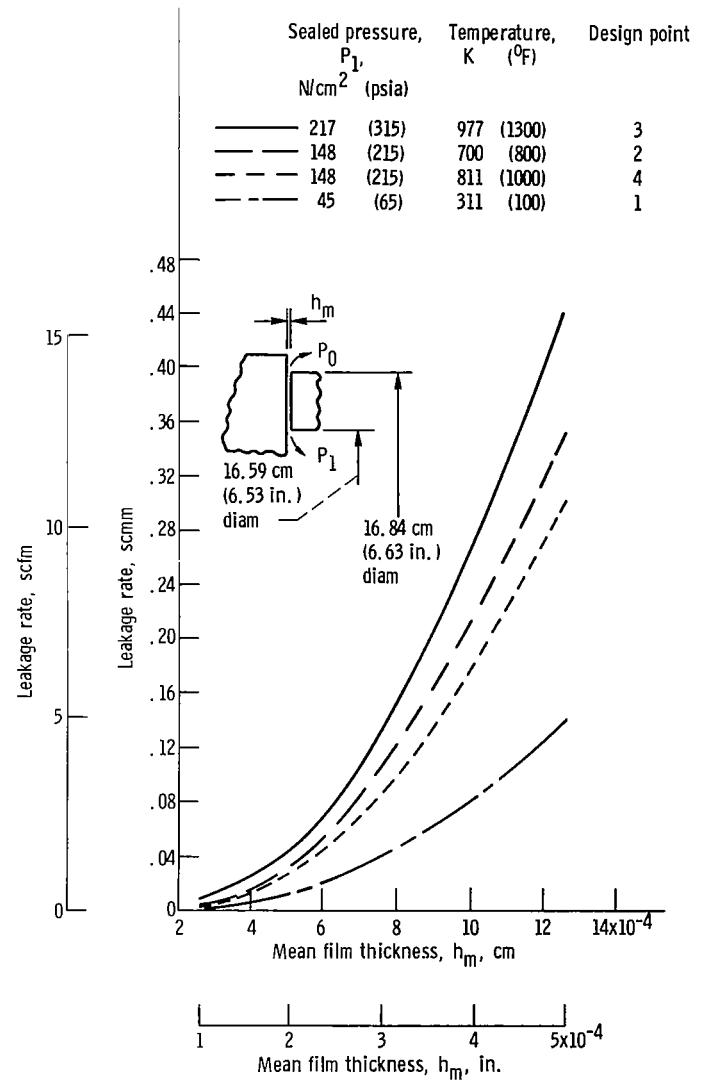
Figure 10. – Leakage rate as function of film thickness. Fluid, air; sump pressure P_0, 10.3 N/cm^2 abs (15 psia); parallel faces.
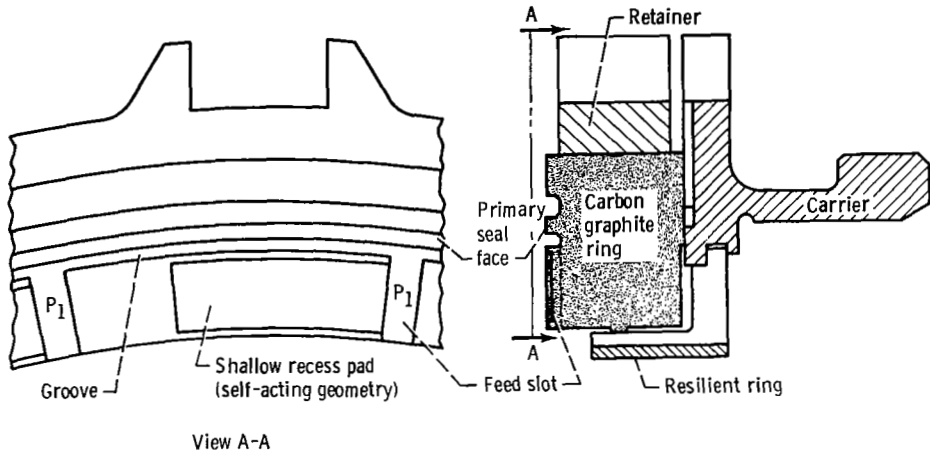
Figure 11. - Self-acting seal with pads on primary ring.
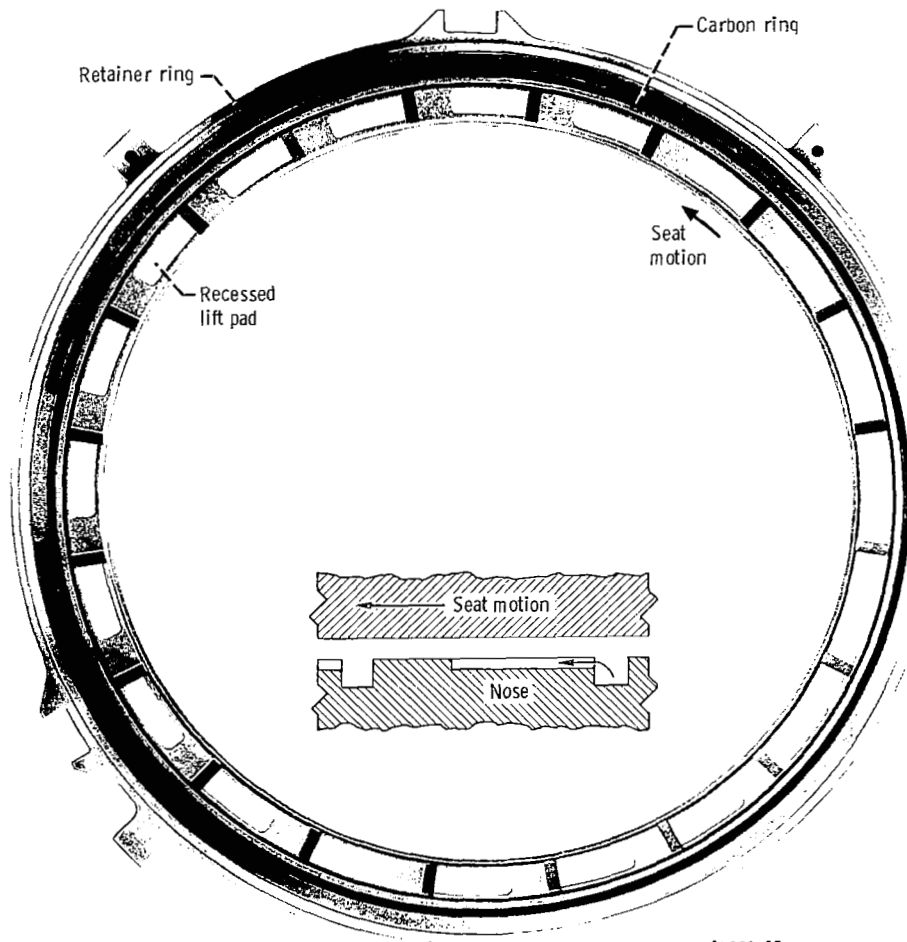
CD-10882-15

Figure 12. - Primary ring assembly.
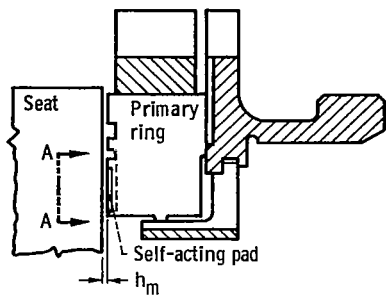
(a) Self-acting pad location.

View A-A

View B-B
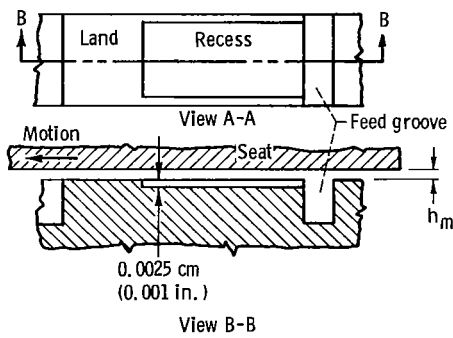
0.0025 cm
(0.001 in.)

(b) Mathematical model of self-acting pad with curvature effects neglected.

Figure 13. – Self-acting pad.

Sliding speed, m/sec (ft/sec)		Temperature, K (°F)		Design point
137	(450)	977	(1300)	3
153	(500)	700	(800)	2
122	(400)	811	(1000)	4
61	(200)	311	(100)	1
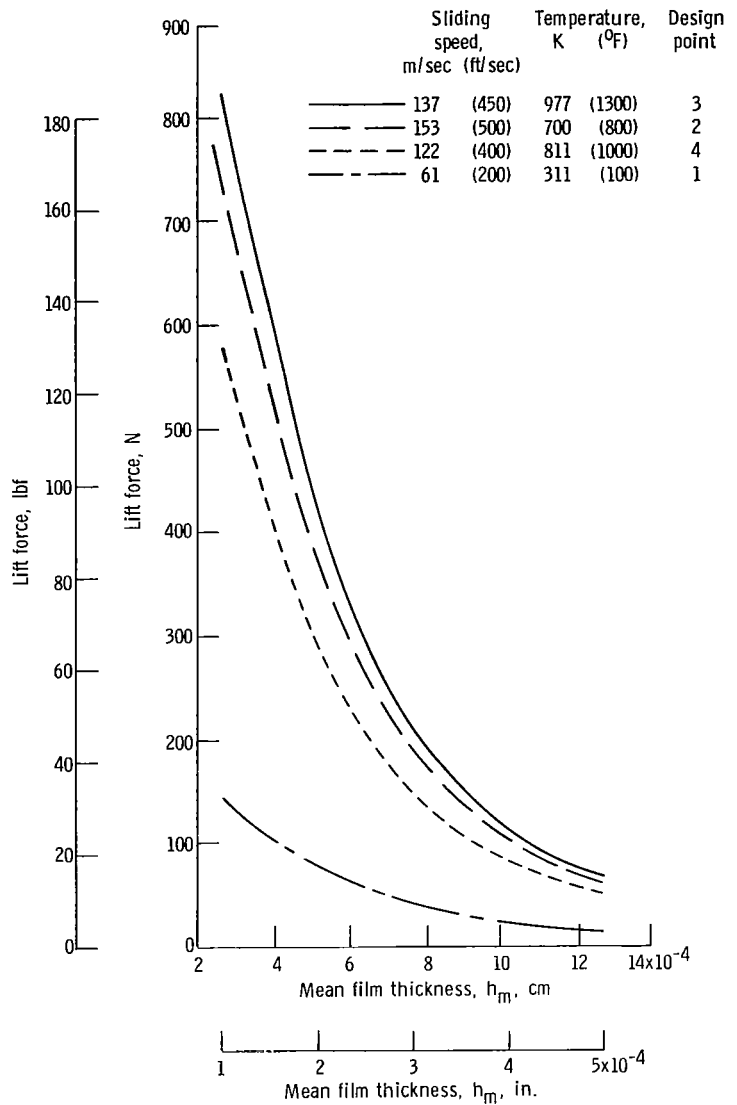
Figure 14. – Lift force of self-acting geometry. Number of pads, 20; recess depth, 0.0025 centimeter (0.001 in.); fluid, air; parallel faces.

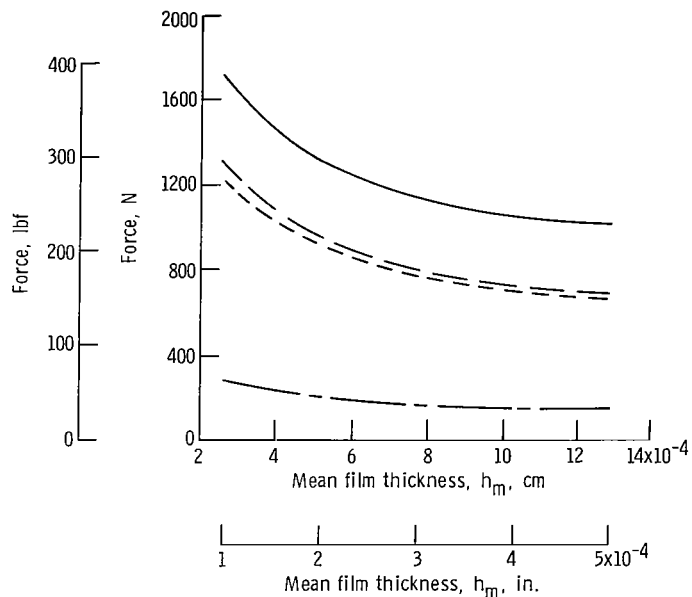| Sealed pressure, P_1		Sliding speed,		Temperature,		Design point
N/cm^2	(psia)	m/sec	(ft/sec)	K	(°F)	
217	(315)	137	(450)	977	(1300)	3
148	(215)	153	(500)	700	(800)	2
148	(215)	122	(400)	811	(1000)	4
45	(65)	61	(200)	311	(100)	1

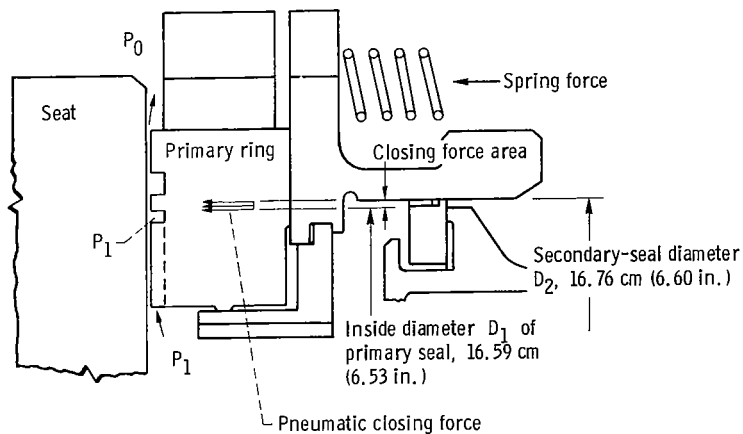Figure 15. - Total opening force - self-acting pad lift force plus primary seal pneumatic force.

Figure 16. - Closing forces - spring force and net closing force due to sealed pressure.

Figure 17. - Calculated temperature field of nosepiece assembly. Design conditions: sealed pressure, 114 N/cm^2 abs (165 psia); mean sliding speed, 153 meters per second (500 ft/sec); sealed gas temperature, 700 K (800° F); oil sump temperature, 461 K (300° F). Temperatures are in K. (From ref. 4.)

* Gas temperature
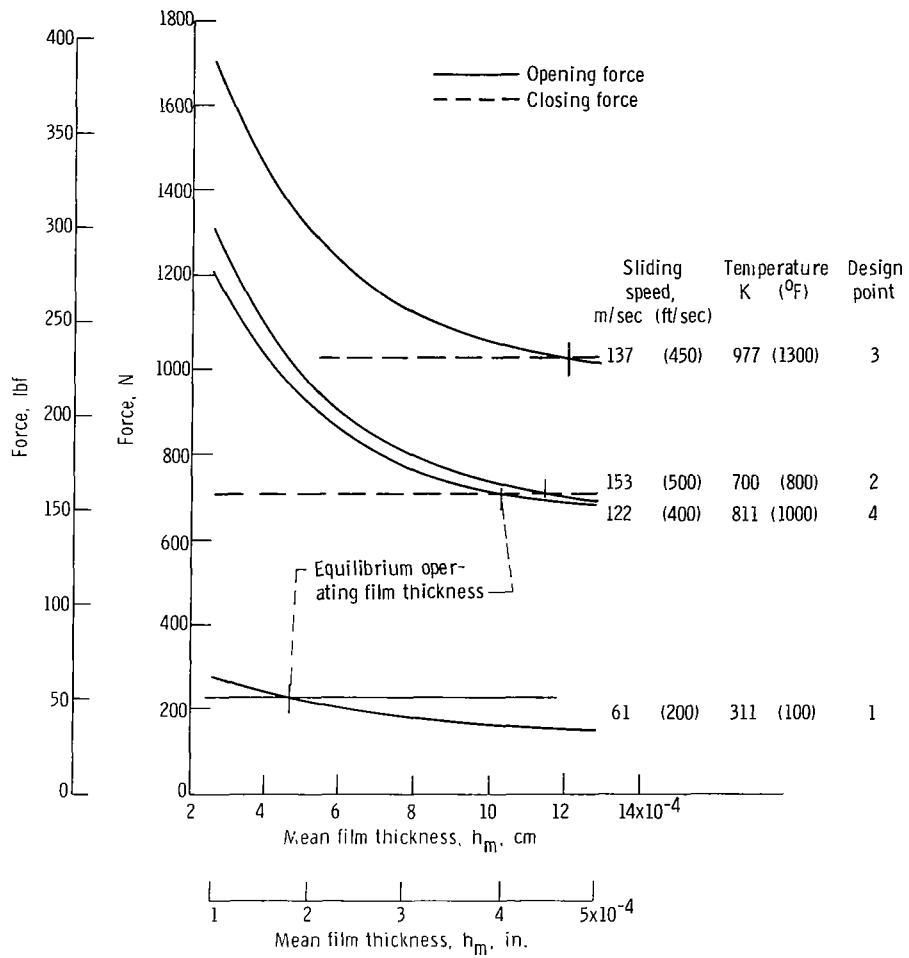
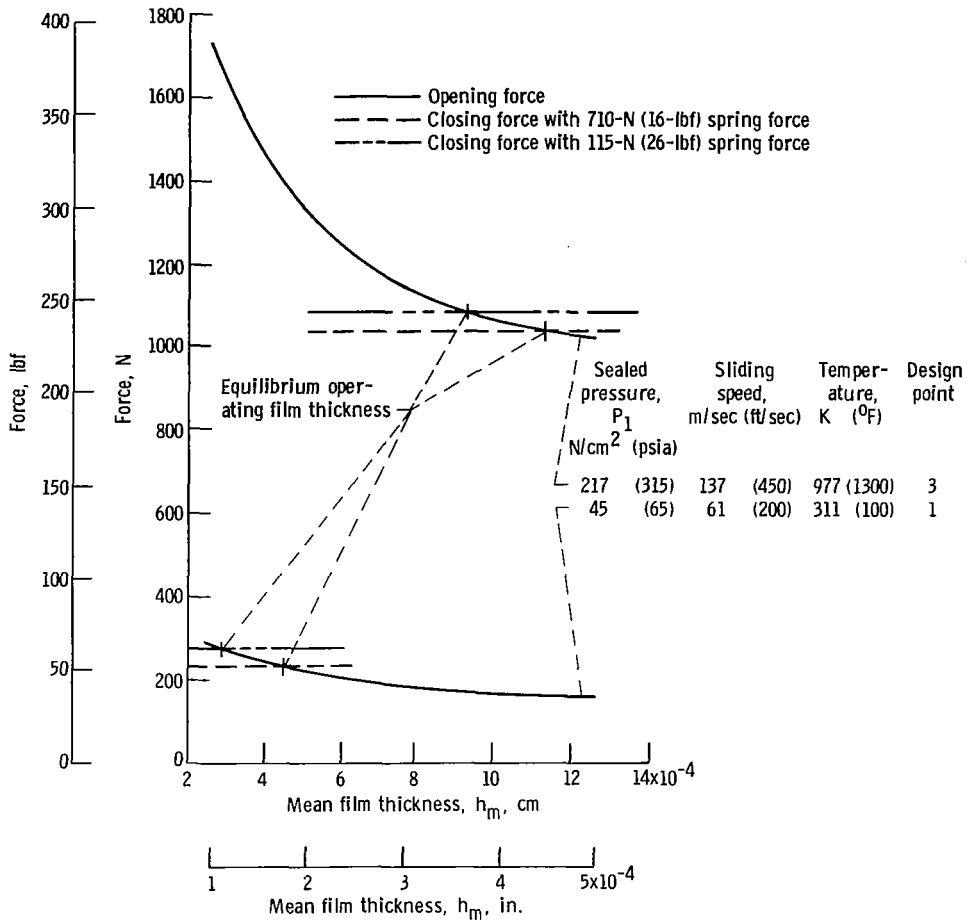Figure 18. - Equilibrium gas film thickness as determined by total seal opening and closing forces. Parallel faces.

Figure 19. - Effect of spring force change on calculated gas film thickness. Design points 1 and 3; parallel faces.
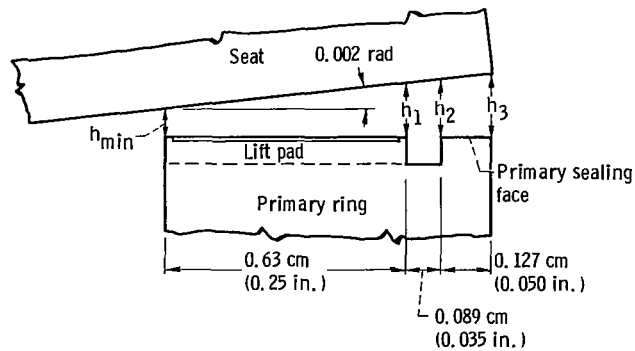
Figure 20. - Two-milliradian deformation of seal seat causing nonparallel faces in primary seal.
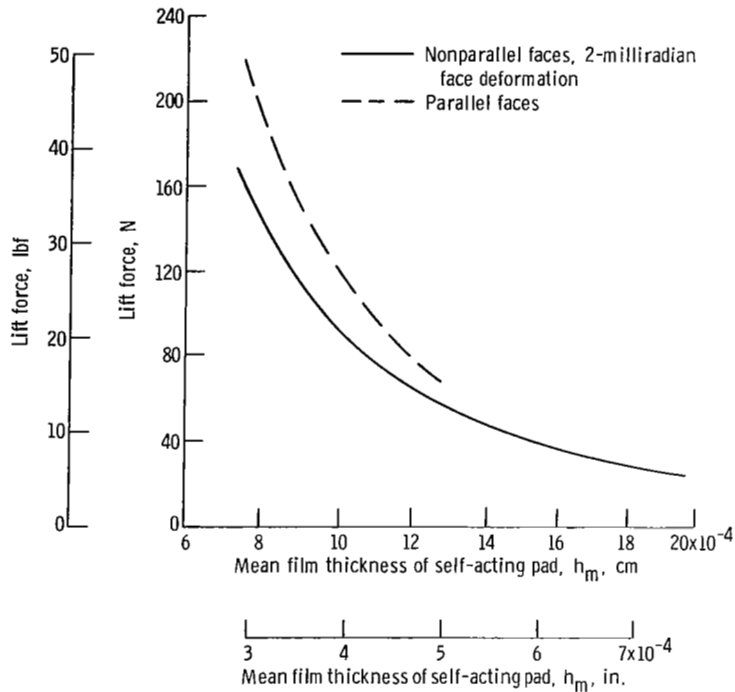
Figure 21. - Lift force of self-acting geometry. Number of pads, 20; pad depth, 0.0025 centimeter (0.001 in.); fluid, air. Design point 2: sealed pressure, 148 N/cm^2 abs (215 psia); sliding speed, 153 meters per second (500 ft/sec); fluid temperature, 700 K (800^0 F).
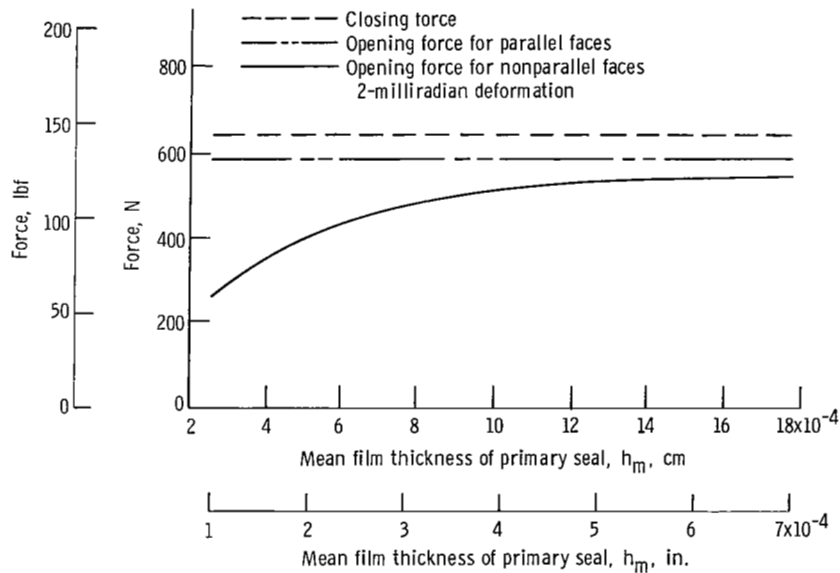

Figure 22. - Sealed pressure forces acting on primary ring assembly. Sealed fluid, air. Design point 2: sealed pressure, 148 N/cm^2 (215 psia); fluid temperature, 700 K (800^0 F).
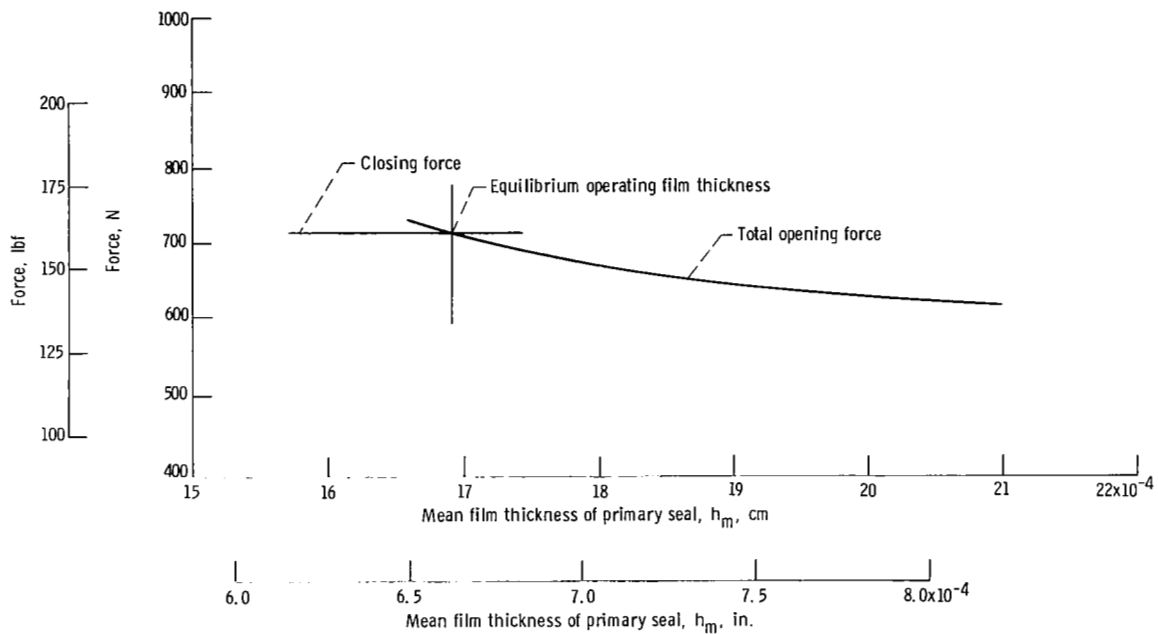
Figure 23. - Equilibrium gas film thickness as determined by total opening and closing forces for 2-milliradian face deformation. Design point 2: sliding speed, 153 meters per second (500 ft/sec); sealed pressure, 148 N/cm^2 abs (215 psia); sealed gas temperature, 700 K (800^0 F).